

Mechanical Characterization of APA Microcapsules by Parallel-Plate Compression

Kiyoshi Bando^{1,*} and Yohei Yamaguchi²

¹Department of Mechanical Engineering, Kansai University, 3-3-35 Yamate-cho, Suita, Osaka 564-8680, Japan

²Graduate School of Kansai University, 3-3-35 Yamate-cho, Suita, Osaka 564-8680, Japan

Abstract: We produced microcapsules of alginate-poly(L)lysine-alginate (APA) with diameters on the order of 10 μm . To characterize their mechanical properties, we conducted an experiment on the parallel-plate compression of a microcapsule and modeled its deformation. In the modeling task, the microcapsule was assumed to be a spherical liquid-filled elastic membrane with negligible bending stiffness and permeability. The membrane thickness was estimated by applying Reissner's linear elastic theory to the experimental force-displacement relationship during loading in the small displacement region. The initial stretch of the membrane was taken into account; it was mainly caused by the osmotic pressure difference across the membrane. The initial stretch of the microcapsule was determined by fitting the calculated and experimental force-displacement relationships during loading at small to medium displacements. At large displacements, the calculated force was smaller than the experimentally measured force because of fluid permeation across the APA membrane. The calculated and experimentally imaged shapes of the deformed microcapsule were compared. The effects of varying the membrane thickness on the force-displacement and transmural pressure-displacement curves were shown, and the limitations of applying the present deformation model were examined.

Keywords: Microcapsule, compression, modeling, mechanical characterization, initial stretch.

1. INTRODUCTION

Microcapsules used for medical applications, such as drug delivery, cell encapsulation, and artificial organs, are highly deformed in blood vessels and in tissues by mechanical stresses or osmotic pressures. Under these loads, the mechanical properties of a microcapsule predominantly affect its deformation behavior; in addition, they govern its stability, burst limit, and adhesion characteristics [1-3]. Therefore, characterizing the mechanical properties of microcapsules is important to control and improve their design for medical applications.

Several experimental methods have been used for determining the mechanical properties of microcapsules: micropipette aspiration [4, 5], atomic force microscopy (AFM) [6-8], optical tweezers [9, 10], magnetic tweezers [11], microfluidic channels [12], and poking [13-15]. Another widely used method is parallel-plate compression [16-21]. In this method, the absence of any locally high-stress region in the membrane allows a microcapsule to undergo large overall deformation. In contrast, when a sharp indenter is used in the poking method, which is considered a model of cell microinjection by using a micropipette, the stress concentration near the sharp edge triggers a rupture of the membrane in a small deformation range.

In a previous report [21] in which APA microcapsules with diameters of 200–300 μm were compressed between parallel plates, we proposed a mechanical model of deformation, assuming that Young's modulus of the membrane was known by an AFM-based method that uses Hertz contact theory [22]. APA microcapsules have been widely used for cell therapy and cell culture [23, 24]. In mechanically modeling parallel-plate compression [21], we assumed a uniform membrane tension; this assumption enabled us to use a practical method for mechanical characterization within an acceptable level of prediction accuracy. In the present report, we applied the compressive deformation model, which improves upon the model in [21] by taking into account an appropriate initial stretch of the membrane, to APA microcapsules (approximately 10 μm in diameter) much smaller than those used previously (200–300 μm in diameter) [21]. The microcapsules were produced from microbeads on the same order of scale, which were generated by the electrohydrodynamic (EHD) spraying method [25, 26].

In several experiments, a microcapsule was compressed between parallel plates made of micropipettes whose tips were melted and formed into flat planes. The small scale of the microcapsule made it difficult to measure the membrane thickness. Then we estimated the thickness by applying the linear elastic theory for a point-force indentation to a spherical shell [27, 28]; that is, the linear theory was adapted to the experimental force-displacement relationship in a small

*Address correspondence to this author at the Department of Mechanical Engineering, Kansai University, 3-3-35 Yamate-cho, Suita, Osaka 564-8680, Japan; Tel: 81-6-6368-1121 Ext. 5813; E-mail: bando@kansai-u.ac.jp

deformation range to obtain the thickness. Similar estimation of thickness with the aid of finite element method (FEM) analysis was reported [29]. The validity of the estimation method was confirmed by applying the method to a larger microcapsule whose membrane thickness was easily measured with a microscope.

In the deformation model, we assumed axisymmetric deformation of an elastic impermeable membrane with negligible bending stiffness and a constant internal volume. The initial stretch of the membrane was determined by fitting the calculated force-displacement curve to the experimental force-displacement relationship, while taking into account the membrane permeability. It was shown that the osmotic pressure of the microcapsule could be estimated by the initial stretch. We discuss the effects of varying the membrane thickness on the force-displacement curve and transmural pressure, the latter of which is directly relevant to the fluid permeation across the membrane.

2. EXPERIMENTS AND ANALYSIS

Alginate gel particles approximately 10 μm in diameter were produced by the electrohydrodynamic spraying method [25, 26, 30]. The breakup of a charged meniscus of sodium alginate solution in the cone-jet mode gave rise to fine droplets, which were sprayed down into a calcium chloride solution to form gel particles of calcium alginate.

APA microcapsules were produced following the method in [23]. The calcium alginate gel particles were immersed in a 0.1 wt% poly(L)lysine solution for 30 min, after which they were immersed in a 1.5 wt% sodium alginate solution for 5 min. The particles were then immersed in a 55 mM sodium citrate solution for 24 h to liquefy the inside of the membrane, resulting in microcapsules with a three-layered alginate-poly(L)lysine-alginate membrane at the surface. A visualized image of the produced microcapsules is shown in Figure 1.

A flat-tip micropipette for compressing a microcapsule of approximately 10 μm in diameter was fabricated as follows. First, a straight glass tube whose inner and outer diameters were 0.69 and 1.19 mm, respectively, (Drummond Scientific Co.) was prepared. A part of it was locally melted by heating, and thinned and cut by stretching in the axial direction with a micropipette tension (MPT-1, Shimadzu Co.). The hollow tip was stemmed by melting with a micropipette furnace (MPF-1, Shimadzu Co.) and then ground into a flat surface with a grinder (EG-400, Narishige Co.).

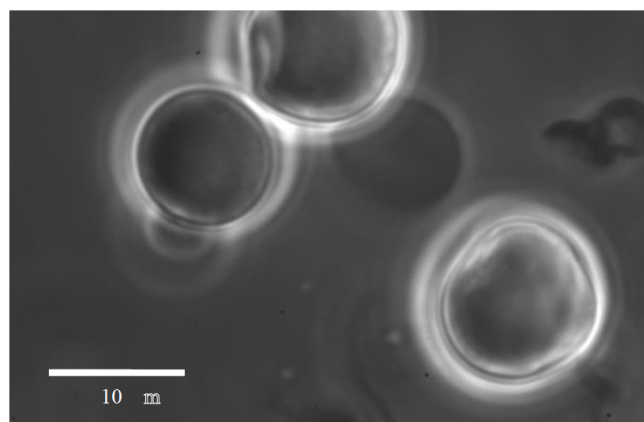


Figure 1: Fabricated alginate-poly(L)lysine-alginate microcapsules of approximately 10 μm in diameter.

As shown in Figure 2, a micromanipulator system (TransferMan NK-2, Eppendorf Co.) was used to test the compression of microcapsules. A flat-tip micropipette was connected to one arm of the manipulator and another flat-tip micropipette was attached to a brass cantilever, which in turn was connected to the other arm of the manipulator. A microcapsule was compressed between the two parallel flat tips of the micropipettes as follows. The upper micromanipulator was moved downward (loading) and then upward (unloading) at a constant speed of approximately 2 $\mu\text{m}/\text{s}$ (Figure 2). During compression experiments, the microcapsule was immersed in a normal saline solution. The shape of the deformed microcapsule and deflection of the cantilever were monitored, using a CMOS camera (DMK 22BUC03, The Imaging Source Co.) through an

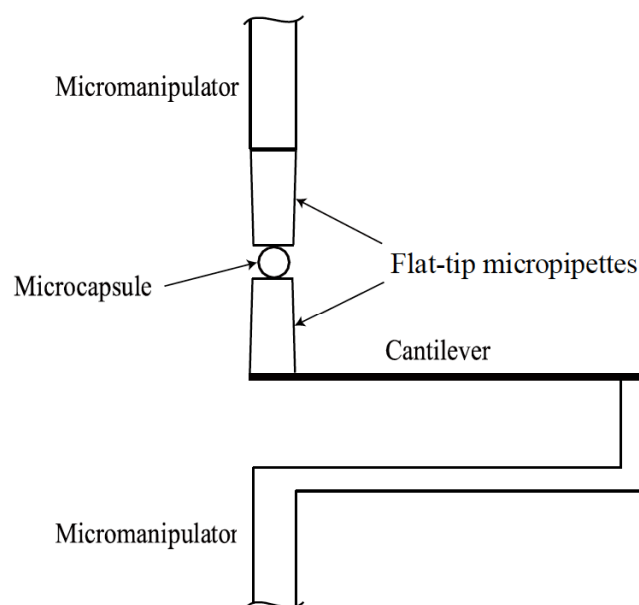


Figure 2: Micromanipulator system for flat-plate compression of a microcapsule.

inverted phase-contrast microscope (IX-70, Olympus Co.). The force applied to the microcapsule was determined as the product of the deflection of the cantilever and the cantilever stiffness.

For microcapsules whose diameters were 200–300 μm , a confocal laser microscope enabled measurement of the membrane thickness observed on the cross-section of a microcapsule embedded in gelatin. However, this method was not applicable to the small microcapsules of the present study.

We estimated the membrane thickness by using the force-displacement curve measured in a microcapsule compression experiment. According to [27, 28], the force-displacement relationship derived from a linear elastic theory of a point force applied to the pole of a spherical shell is expressed as

$$F = \frac{4Eh^2}{\sqrt{3(1-\nu^2)}} \left(\frac{\delta}{R_0} \right) \quad (1)$$

where F is the applied force, δ is the displacement, E is Young's modulus, h is the membrane thickness, ν is the Poisson ratio, and R_0 is the radius. The experimental force-displacement relationship for parallel-plate compression of an APA microcapsule with a diameter of 240 μm is shown in Figure 3 [21]. Young's modulus of the membrane was measured as 1.9 MPa by the AFM-based method under the assumed Poisson ratio of 0.5 [22], and the membrane thickness measured with a microscope was 7.75 μm . The straight line in Figure 3 shows Eq. (1), whose slope $4Eh^2/\sqrt{3(1-\nu^2)}$ is calculated from the data denoted above. The open and filled circles correspond to the experimental loading and unloading phases, respectively. The hysteresis between loading and unloading was caused by fluid permeation across the APA membrane [21], although the permeability effect is negligible when the displacement is small during loading. In Figure 3, the straight line derived from Reissner's theory, in which the permeability is not taken into account, is in good agreement with the open circles at small displacements. Therefore, when the values of E and ν are known, h can be estimated by fitting the tangent line to the experimental force-displacement relationship during loading at small displacements. Although Eq. (1) is derived for the compression of a point force, it is applicable to flat-plate compression in the small displacement region by virtue of the small contact region between the plate and membrane. A similar method to estimate the membrane thickness with the aid of FEM analysis was reported in [29].

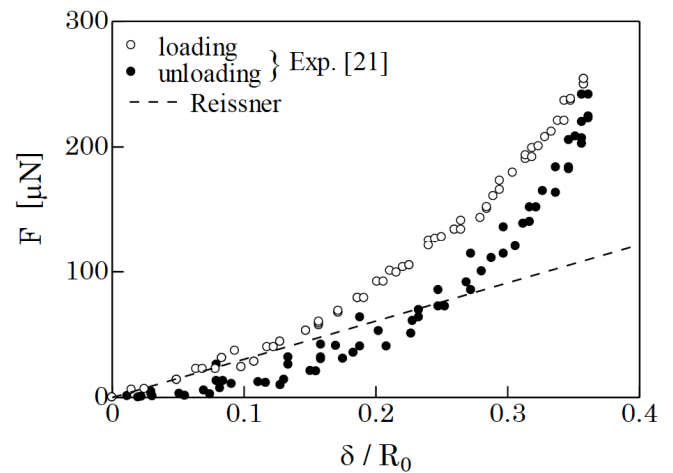


Figure 3: Force-displacement relationship for an APA microcapsule of 240 μm in diameter.

A compression experiment was performed for a microcapsule of 8.8 μm in diameter, using the micromanipulator system shown in Figure 2. The measured force-displacement relationship is shown by the open (loading) and filled (unloading) symbols in Figure 4. The tangent line from the origin to the open circles in the small displacement region is shown by the broken line. Young's modulus of the membrane, as measured by an indentation test with the AFM-based method, was $E = 0.58$ MPa under the assumed Poisson ratio of $\nu = 0.5$. By entering the slope of the broken line in Figure 4 and the above values of E and ν into Eq. (1), we obtain a thickness of $h = 1.22$ μm .

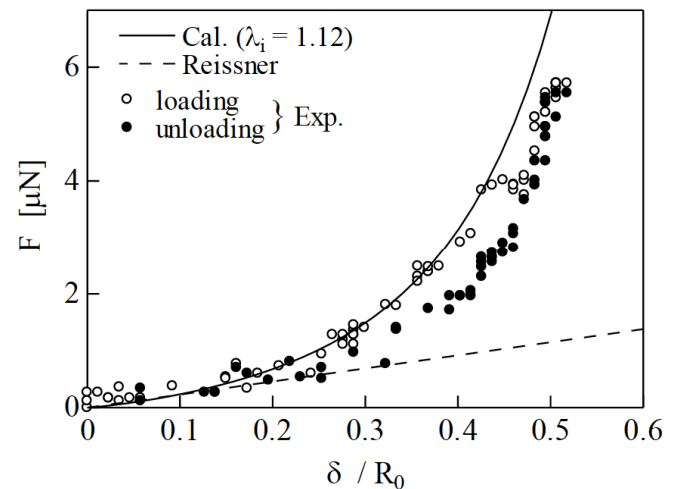


Figure 4: Force-displacement relationship for an APA microcapsule of 8.8 μm in diameter.

3. DEFORMATION MODEL

The microcapsules preserved after production and those in the compression experiment were immersed in a normal saline solution. The diameter of a microcapsule in the preserved state and in the initial state of compression is assumed to be R_0 . The initial

stretch of the membrane is $\lambda_i (= R_0 / R_i)$, which denotes the initial expansion from a radius of R_i due mainly to the osmotic pressure difference across the membrane. The microcapsule is compressed by two parallel plates and its deformed shape is assumed to be axisymmetric. The meridional shapes of the microcapsule in the tension-free, expanded, and deformed states are shown in cylindrical coordinates (r, z) in Figure 5. Only one half of the microcapsule is modeled given its equatorial symmetry. The displacement of the flat plate from the point of contact inception is denoted by δ . The coordinate s is taken along the deformed contour, in which the equator point and contact point are denoted by 1 and 2, respectively. The outward normal to the deformed surface is denoted by n and the angle between directions n and r by α .

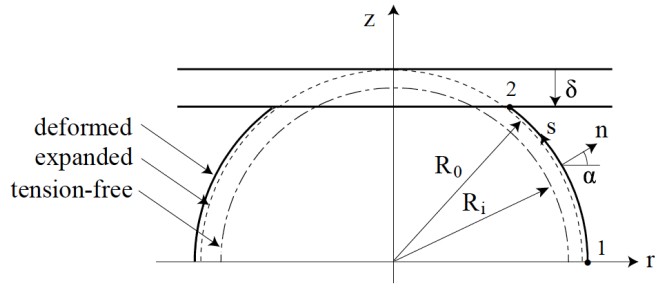


Figure 5: Calculation models for a microcapsule under tension-free, expanded, and deformed conditions.

The static equilibrium equations of the forces for an axisymmetric membrane with negligible bending stiffness in the meridional tangential and normal directions are, respectively, expressed by [31]

$$\frac{dT_s}{ds} + \frac{1}{r} \frac{dr}{ds} (T_s - T_\varphi) = 0 \quad (2)$$

$$\kappa_s T_s + \kappa_\varphi T_\varphi = p_{tr} \quad (3)$$

where T_s and T_φ are the principal stress resultants (tensions). κ_s and κ_φ are the principal curvatures in the meridional and orthogonal planes, respectively, and p_{tr} is the net (internal minus external) transmural pressure. The principal curvatures are expressed by

$$\kappa_s = \frac{d\alpha}{ds}, \quad \kappa_\varphi = \frac{\cos\alpha}{r} \quad (4)$$

For simplicity we assume that $T_s = T_\varphi$ [21]. The following equations are then obtained from Eqs. (2)–(4).

$$\cos\alpha = \frac{C}{2}r + \frac{D}{r} \quad (5)$$

$$T = \frac{p_{tr}}{C} \quad (6)$$

where T is a uniform tension, and C and D are constants expressed by

$$C = \frac{2r_1}{r_1^2 - r_2^2}, D = \frac{r_1 r_2^2}{r_2^2 - r_1^2} \quad (7)$$

The values of r_1 and r_2 are determined so that the following two conditions are satisfied.

The first condition is that the volume of the liquid-filled microcapsule is constant during deformation and is expressed by

$$\frac{2\pi}{3} \int_{s_1}^{s_2} r(n_r r + n_z z) ds + \frac{\pi}{3} r_2^2 z_2 = V_0 \quad (8)$$

where $V_0 (= 2\pi R_0^3 / 3)$ is the volume just before compression, and n_r and n_z are the r - and z -components, respectively, of the outward unit vector normal to the membrane surface. The constancy of the volume is consistent with the assumption that the permeability of the membrane is ignored.

The second condition is the equilibrium of forces in the z -direction applied to the half-model of the microcapsule as shown in Figure 5, which is expressed by

$$F + 2\pi r_1 T - \pi r_1^2 p_{tr} = 0 \quad (9)$$

where F is the compression force from the flat plate.

The area strain of the membrane is defined as

$$\varepsilon_a = \frac{A - A_i}{A_i} \quad (10)$$

where $A_i (= 2\pi R_i^2)$ is the membrane area in the tension-free state, and A is the area of the deformed membrane, which is calculated by

$$A = 2\pi \int_{s_1}^{s_2} r ds + \pi r_2^2 \quad (11)$$

The tension T is calculated from the area elastic modulus K and the area strain as follows.

$$T = K\varepsilon_a \quad (12)$$

The area elastic modulus is calculated by [32]

$$K = \frac{Eh}{2(1-\nu)} \quad (13)$$

Substituting Eqs. (6) and (12) into Eq. (9), we obtain

$$F + \pi r_1^2 (2 - Cr_1) K \varepsilon_a = 0 \quad (14)$$

The calculation procedure to obtain the deformed shape and the relationship between the compression force and displacement of the plate is as follows.

[1] Assign F . [2] Assume r_1 and r_2 and then evaluate C and D in Eq. (7) [3]. Calculate the deformed shape by using Eq. (5). [4]. Iterate procedures [2, 3] until Eqs. (8) and (14) are satisfied. The iteration procedures [2, 3] were performed by the Newton method, in which the Jacobian matrix of 2×2 was calculated numerically.

4. RESULTS AND DISCUSSION

The initial stretch λ_i is caused by the initial transmural pressure $p_{tr,i}$, which for a spherical membrane is expressed by

$$p_{tr,i} = \frac{2K(\lambda_i^2 - 1)}{R_0} \quad (15)$$

This equation is derived from the Laplace equation [32]. In the numerical calculation of the flat-plate compression of a microcapsule with an initial stretch, the initial transmural pressure is calculated as the limiting value of a small compression force divided by a small contact area between the flat plate and microcapsule surface. The deformed shape caused by a small force due to flat-plate compression is approximated by a sphere. In Figure 6, the calculation results for a small value of $F = 0.01 \mu\text{N}$, shown by the black circles, are in good agreement with the values obtained from Eq. (15). The black circles in Figure 6

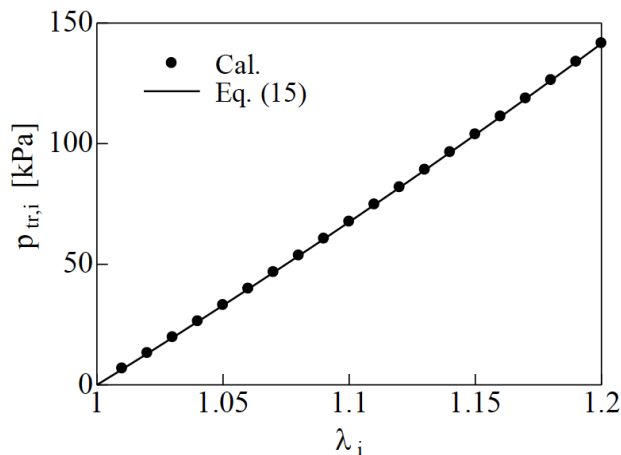


Figure 6: Comparison of calculation results and Eq. (15) for relationship between initial transmural pressure and initial stretch.

were plotted by calculating the value of $p_{tr,i} (= F / \pi r_2^2)$ with the variation of the initial stretch λ_i . This result validates the present calculation method in the small deformation range.

In the force-displacement relationship of Figure 4, the open and filled circles show the experimental results during loading and unloading, respectively. The hysteresis between the open and filled circles was caused by fluid permeation across the membrane of the APA microcapsule. This was confirmed by calculating the volume of the measured microcapsule under the assumption of axisymmetric deformation. The solid line shows the calculation result, which is fitted to the open circles in the small and medium displacement regions by adjusting the value of the initial stretch λ_i . At large displacements, the microcapsule was compressed strongly and the increased internal pressure induced a large amount of fluid to permeate outward. It follows that the compression force decreases in the large displacement region and the open circles deviate from the solid line (Figure 4). The reduction in compression force as a result of the membrane permeability was reported in [20]. The initial stretch determined by the above procedure was 1.12. The initial transmural pressure, which is mainly attributed to the osmotic pressure difference across the microcapsule membrane, is then calculated by Eq. (15). Owing to the small scale of the microcapsules (on the order of $10 \mu\text{m}$), measuring the inside osmotic pressure is difficult. In one method, the liquid inside of plant cells was extracted using a micropipette and the osmotic pressure was measured by freezing point depression [33]. The assumption of $T_s = T_\varphi$ was used to simplify the basic equations. The difference between T_s and T_φ was evaluated in [34], in which the assumption was not used. The validity of the assumption is partly shown by the agreement of the solid line and the open circles in Figure 4.

The compression experiments, which were performed to approximately 50% fractional displacement, showed no membrane rupture in the compression range. On the other hand, membrane rupture was observed for APA microcapsules of 200–300 μm in diameter at nearly 50% of fractional displacement [21], in which the diameter-to-thickness ratio was 31. This ratio for the APA microcapsule of $8.8 \mu\text{m}$ in diameter in the present study was smaller (7.2); therefore, the present microcapsule was more resistant against membrane rupture.

Figure 7 shows a comparison of the microcapsule shapes between the calculation results (broken red lines) and the experimentally visualized images for the

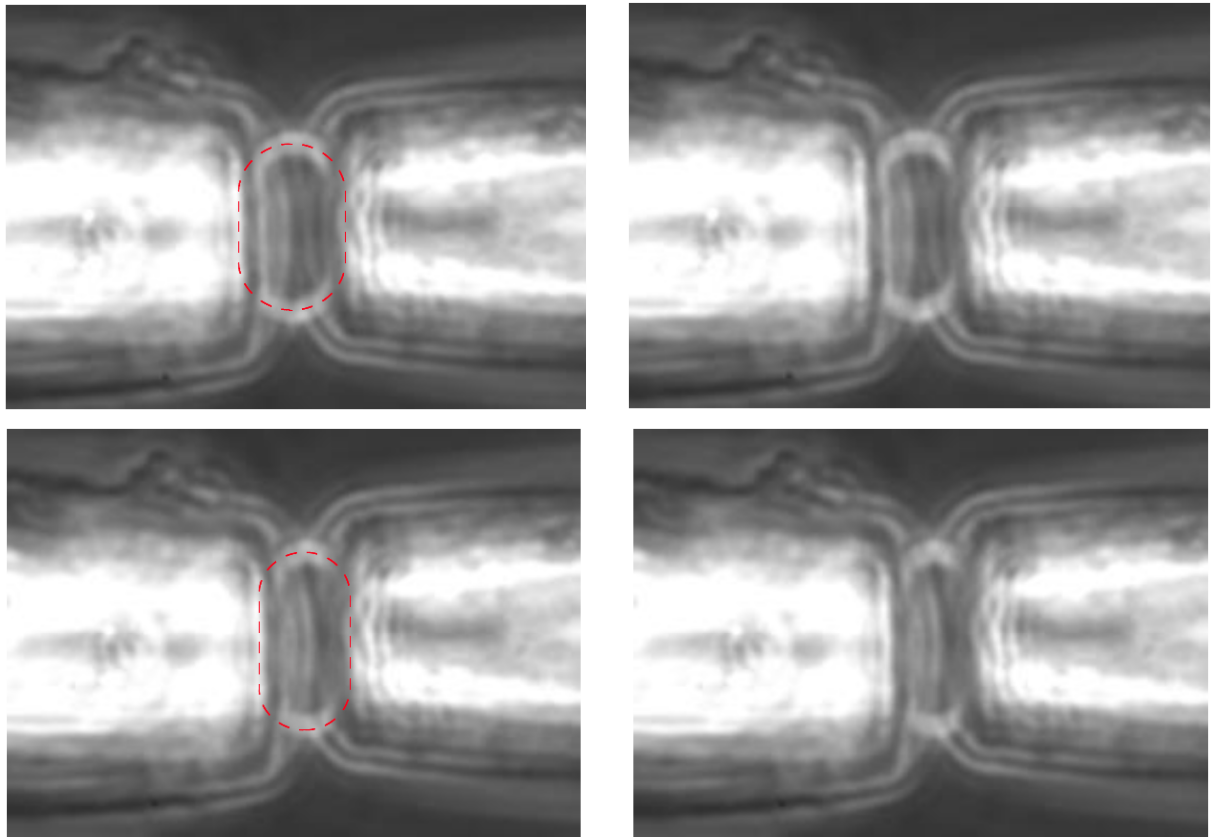


Figure 7: Comparison of deformed shapes between calculated (broken red lines) and experimental results for $\delta/d_0 = 0.29$ (top) and 0.40 (bottom) during loading.

case where the fractional displacement was 0.29 (top) or 0.40 (bottom) during loading. The two images on the right-hand side in Figure 7 are the same as the two images on left-hand side. In the images on the right-hand side, the calculated lines are removed for ease of comparison. The bright blurred contours of the microcapsules are caused by the halo effect, an optical artifact related to the phase-contrast microscope [35]. The calculated and experimentally visualized shapes are almost identical at the round portions of the microcapsule contour, although the straight portions of experimentally visualized contour are unclear due to the halo effects at the contact areas between the microcapsule surface and micropipette tips.

Figure 8 shows the effects of varying the membrane thickness on the force-displacement curve. The solid lines show the calculation results of the present deformation model and the broken lines show results obtained by Reissner’s theory. An increase in thickness increases the compression force, indicating that microcapsule rigidity increases with increasing thickness. The slopes at the origin of the force-displacement curves for the present model agree well with the linear theory for thicknesses of $h = 0.6$ (Figure 8) and $1.22 \mu\text{m}$ (Figure 4). However, a discrepancy

between the slopes at the origin is seen for the case of $h = 1.8 \mu\text{m}$, in which the diameter-to-thickness ratio is 4.9 . This case is apparently beyond the scope of application not only for the present model but also for Reissner’s theory.

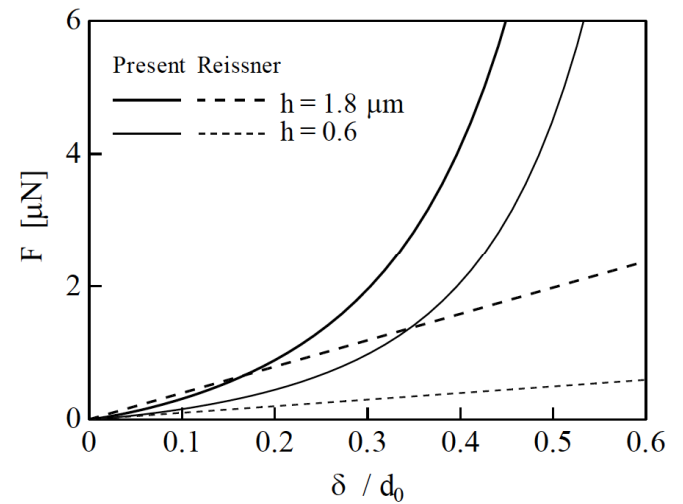


Figure 8: Effect of varying membrane thickness on force-displacement relationship.

Figure 9 shows the effects of varying the thickness on the transmural pressure p_{tr} . The transmural

pressure rises as the membrane thickness increases. The increase in transmural pressure causes outward fluid permeation across the membrane. When the membrane is thin (e.g., $h = 0.1 \mu\text{m}$), the transmural pressure remains almost constant, resulting in very little fluid permeation. In the case of $h = 1.22 \mu\text{m}$, as in the present experiment, the transmural pressure increases in the large displacement region, resulting in the divergence between the solid line and open circles in Figure 4. This is because membrane permeability is not incorporated into the present membrane model.

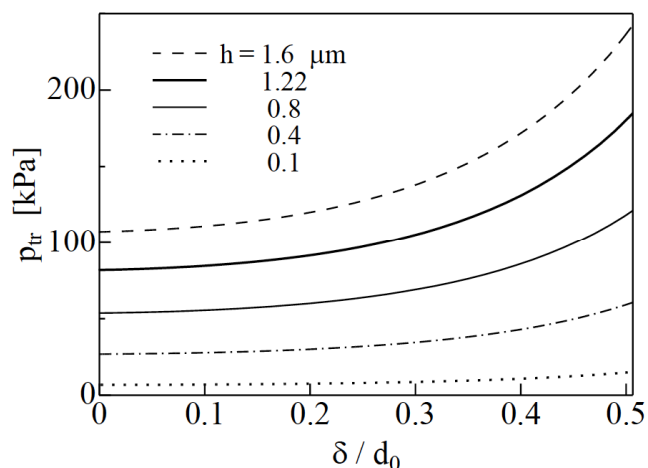


Figure 9: Effect of varying membrane thickness on transmural pressure-displacement relationship.

Calculation results relevant to the effects of membrane thickness showed that microcapsule rigidity and permeability can be controlled by varying the membrane thickness. The thickness of the APA microcapsule membrane could be adjusted by changing experimental conditions in the production process, such as the concentration of sodium alginate, the concentration of poly(L)lysine, the reaction time with poly(L)lysine, the molecular weight of poly(L)lysine, and the treatment time for the second coating of sodium alginate [36].

5. CONCLUSIONS

APA microcapsules with diameters on the order of $10 \mu\text{m}$ were produced from microbeads generated by utilizing the cone-jet mode in EHD spraying. We proposed a method to characterize the mechanical properties of the microcapsule. The characterized properties were Young's modulus, the thickness, and the initial stretch of the membrane. Young's modulus of the membrane was determined by the AFM-based method under the assumption of a Poisson ratio of 0.5. Experiments on flat-plate compression of the microcapsule were performed. The thickness of the membrane was obtained by applying Reissner's linear

elastic theory for point-force indentation of a spherical shell to the experimental force-displacement relationship during loading in the small displacement region. The initial stretch of the membrane was determined by fitting the calculated force-displacement curve to the experimental force-displacement relationship in the small and medium displacements regions during loading. The osmotic pressure difference across the membrane can be estimated from the obtained initial stretch. When the rigidity and permeability of the microcapsule are adjusted, a promising method is to change the membrane thickness. The present method is practical and effective for the mechanical characterization of microcapsules.

ACKNOWLEDGEMENTS

This research was partly financially supported by the Kansai University Grant-in-Aid for progress of research in graduate course, 2017.

REFERENCES

- [1] Liu KK. Deformation behaviour of soft particles: a review. *J Phys D* 2006; 39: R189-R199. <https://doi.org/10.1088/0022-3727/39/11/R01>
- [2] Fery A, Weinkamer R. Mechanical properties of micro- and nanocapsules: Single-capsule measurements. *Polymer* 2007; 48: 7221-7235. <https://doi.org/10.1016/j.polymer.2007.07.050>
- [3] Mercadé-Prieto R, Zhang Z. Mechanical characterization of microspheres - capsules, cells and beads: a review. *J Microencapsulation* 2012; 29: 277-285. <https://doi.org/10.3109/02652048.2011.646331>
- [4] Needham D, Zhelev DV. The mechanochemistry of lipid vesicles examined by micropipet manipulation techniques. In: Rosoff M, Ed. *Vesicles*. New York: Marcel Dekker 1996; 373-444.
- [5] Hochmuth RM. Micropipette aspiration of living cells. *J Biomech* 2000; 33: 15-22. [https://doi.org/10.1016/S0021-9290\(99\)00175-X](https://doi.org/10.1016/S0021-9290(99)00175-X)
- [6] Lulevich VV, Radtchenko IL, Sukhorukov GB, Vinogradova OI. Deformation properties of nonadhesive polyelectrolyte microcapsules studied with the atomic force microscope. *J Phys Chem B* 2003; 107: 2735-2740. <https://doi.org/10.1021/jp026927y>
- [7] Wright CJ, Shah MK, Powell LC, Armstrong I. Application of AFM from microbial cell to biofilm. *Scanning* 2010; 32: 134-149. <https://doi.org/10.1002/sca.20193>
- [8] Ghaemi A, Philipp A, Bauer A, Last K, Fery A, Stephan G. Mechanical behaviour of micro-capsules and their rupture under compression. *Chem Eng Sci* 2016; 142: 236-243. <https://doi.org/10.1016/j.ces.2015.11.002>
- [9] Ashkin A. Optical trapping and manipulation of neutral particles using lasers. *Proc Natl Acad Sci* 1997; 94: 4853-4860. <https://doi.org/10.1073/pnas.94.10.4853>
- [10] Helfer E, Harlepp S, Bourdieu L, Robert J, MacKintosh FC, Chatenay D. Microrheology of biopolymer-membrane complexes. *Phys Rev Lett* 2000; 85: 457-460. <https://doi.org/10.1103/PhysRevLett.85.457>

- [11] Vlaminck ID, Dekker C. Recent advances in magnetic tweezers. *Annu Rev Biophys* 2012; 41: 453-472. <https://doi.org/10.1146/annurev-biophys-122311-100544>
- [12] Lefebvre Y, Leclerc E, Barthès-Biesel D, Walter J. Flow of artificial microcapsules in microfluidic channels: A method for determining the elastic properties of the membrane. *Phys Fluids* 2008; 20: 123102-1-123102-10. <https://doi.org/10.1063/1.3054128>
- [13] Taber LA. Large deflection of a fluid-filled spherical shell under a point load. *J Appl Mech* 1982; 49: 121-128. <https://doi.org/10.1115/1.3161953>
- [14] Tan Y, Sun D, Huang W, Cheng SH. Mechanical modeling of biological cells in microinjection. *IEEE Trans Nanobioscience* 2008; 7: 257-266. <https://doi.org/10.1109/TNB.2008.2011852>
- [15] Bando K, Oiso Y. Indentation analysis of microcapsule with initial stretch. *J Biomech Sci Eng* 2013; 8: 268-277. <https://doi.org/10.1299/jbse.8.268>
- [16] Liu KK, Williams DR, Briscoe BJ. Compressive deformation of a single microcapsule. *Phys Rev E* 1996; 54: 6673-6680. <https://doi.org/10.1103/PhysRevE.54.6673>
- [17] Zhang Z, Blewett JM, Thomas CR. Modelling the effect of osmolality on the bursting strength of yeast cells. *J Biotech* 1999; 71: 17-24. [https://doi.org/10.1016/S0168-1656\(99\)00012-7](https://doi.org/10.1016/S0168-1656(99)00012-7)
- [18] Carin M, Barthès-Biesel D, Edwards-Lévy F, Postel C, Andrei DC. Compression of biocompatible liquid-filled HSA-alginate capsules: Determination of the membrane mechanical properties. *Biotech Bioeng* 2003; 82: 207-212. <https://doi.org/10.1002/bit.10559>
- [19] Risso F, Carin M. Compression of a capsule: Mechanical laws of membranes with negligible bending stiffness. *Phys Rev E* 2004; 69: 061601-1-061601-7. <https://doi.org/10.1103/PhysRevE.69.061601>
- [20] Wang CX, Wang L, Thomas CR. Modelling the mechanical properties of single suspension-cultured tomato cells. *Ann Bot* 2004; 93: 443-453. <https://doi.org/10.1093/aob/mch062>
- [21] Bando K, Ohba K, Oiso Y. Deformation analysis of microcapsules compressed by two rigid parallel plates. *J Biorheol* 2013; 27: 18-25. <https://doi.org/10.1007/s12573-012-0053-8>
- [22] Sneddon IN. The relation between load and penetration in the axisymmetric Boussinesq problem for a punch of arbitrary profile. *Int J Eng Sci* 1965; 3: 47-57. [https://doi.org/10.1016/0020-7225\(65\)90019-4](https://doi.org/10.1016/0020-7225(65)90019-4)
- [23] Okada N, Miyamoto H, Yoshioka T, Katsume A, Saito H, Yorozu K, Ueda O, Itoh N, Mizuguchi H, Nakagawa S, Ohsugi Y, Mayumi T. Cytomedical therapy for IgG1 plasmacytosis in human interleukin-6 transgenic mice using hybridoma cells microencapsulated in alginate-poly(L)lysine-alginate membrane. *Biochim Biophys Acta* 1997; 1360: 53-63. [https://doi.org/10.1016/S0925-4439\(96\)00066-X](https://doi.org/10.1016/S0925-4439(96)00066-X)
- [24] Peirone M, Ross CJD, Hortelano G, Brash JL, Chang PL. Encapsulation of various recombinant mammalian cell types in different alginate microcapsules. *J Biomed Mater Res* 1998; 42: 587-596. [https://doi.org/10.1002/\(SICI\)1097-4636\(19981215\)42:4<587::AID-JBM15>3.0.CO;2-X](https://doi.org/10.1002/(SICI)1097-4636(19981215)42:4<587::AID-JBM15>3.0.CO;2-X)
- [25] Bailey AG. Electrostatic spraying of liquids. New York: Wiley 1988.
- [26] Cloupeau M, Prunet-Foch B. Electrohydrodynamic spraying functioning modes: a critical review. *J Aerosol Sci* 1994; 25: 1021-1036. [https://doi.org/10.1016/0021-8502\(94\)90199-6](https://doi.org/10.1016/0021-8502(94)90199-6)
- [27] Reissner E. Stresses and small displacements of shallow spherical shells. I. *J Math Phys* 1946; 25: 80-85. <https://doi.org/10.1002/sapm194625180>
- [28] Reissner E. Stresses and small displacements of shallow spherical shells. II. *J Math Phys* 1947; 25: 279-300. <https://doi.org/10.1002/sapm1946251279>
- [29] Mercadé-Prieto R, Nguyen B, Allen R, York D, Preece JA, Goodwin TE, Zhang Z. Determination of the elastic properties of single microcapsules using micromanipulation and finite element modeling. *Chem Eng Sci* 2011; 66: 2042-2049. <https://doi.org/10.1016/j.ces.2011.01.015>
- [30] Watanabe T. Production of polymer gel particles by means of electrohydrodynamic (EHD) spraying - Influence of cylindrical grid electrodes surrounding a narrow nozzle on spraying characteristics -. Master's Thesis Kansai Univ 2011.
- [31] Flügge W. Stresses in Shells. Berlin: Springer 1973.
- [32] Evans EA, Skalak R. Mechanics and Thermodynamics of Biomembranes. Florida: CRC Press 1980.
- [33] Tomos D, Hinde P, Richardson P, Pritchard J, Fricke W. Microsampling and measurements of solutes in single cells. In: Harris N, Oparka KJ, eds. *Plant Cell Biology: A Practical Approach*. Oxford: Oxford Univ Press 1994; 297-314.
- [34] Bando K. Compressive deformation analysis of Alginate-Poly(L)lysine-Alginate (APA) microcapsule. *J Biomech Sci Eng* 2013; 1: 40-48. <https://doi.org/10.1299/jbse.8.40>
- [35] Pluta M. *Advanced Light Microscopy*. Vol. 2, Amsterdam: Elsevier 1988.
- [36] Ma X, Vacek I, Sun A. Generation of alginate-poly-L-lysine-alginate (APA) biomicrocapsules: The relationship between the membrane strength and the reaction conditions. *Art Cells Blood Subs Immob Biotech* 1994; 22: 43-69. <https://doi.org/10.3109/10731199409117399>

Received on 14-04-2017

Accepted on 10-05-2017

Published on 04-08-2017

DOI: <https://doi.org/10.6000/1929-6037.2017.06.02.1>

© 2017 Bando and Yamaguchi; Licensee Lifescience Global.

This is an open access article licensed under the terms of the Creative Commons Attribution Non-Commercial License (<http://creativecommons.org/licenses/by-nc/3.0/>) which permits unrestricted, non-commercial use, distribution and reproduction in any medium, provided the work is properly cited.